Distance Dependence of the Electron Transfer Rate through Oligoglycine Spacers Introduced into Self-Assembled Monolayers

Slawomir Sek, Anna Sepiol, Anna Tolak, Aleksandra Misicka, and Renata Bilewicz*

Department of Chemistry, University of Warsaw, Pasteura 1, 02093 Warsaw, Poland

Received: February 27, 2004; In Final Form: May 7, 2004

A series of oligoglycine derivatives (Fc−CO(Gly)$_n$NH−(CH$_2$)$_2$−SH (where Fc = ferrocene; Gly = glycine; $n = 2-6$) were synthesized and then self-assembled on gold in the presence of selected alkanethiols in order to form mixed monolayers. The properties and electron transfer behavior of the monolayer assemblies were investigated using electrochemical methods. It was found that the rates of electron transfer through oligoglycine bridges decrease rapidly with distance only for short chain derivatives, while for the longer bridges the distance dependence is weaker. Differences in the secondary structure of the peptide bridges and the change of the electron transfer mechanism are considered as possible reasons of the increase of the rate constants observed for the longer peptide chains.

Introduction

Despite significant progress in the understanding of long-range charge transport mechanisms, the bridge-mediated electron transfer reactions still belong to the most important and active areas of research.[1−5] In biological systems, electron transfer (ET) reactions often occur across multiple peptide chains, which separate the donor from the acceptor.[6−8] Systematic studies of well-defined donor−bridge−acceptor systems can simplify the analysis of electron transfer pathways in proteins. It has been demonstrated that self-assembled monolayers (SAMs) of thiolated compounds on metal electrodes can serve as useful model systems for the studies of kinetics of mediated electron transfer.[9−16] In our approach, monolayer assemblies of molecules containing amide bonds or oligopeptides are used for the characterization of peptide electron transport properties.[17−20] Electron or hole transfer between given donor and acceptor sites can be modulated by changing the distance or by modifying the structure of the intervening bridge between them.[11−24] In specific cases, as shown recently by Foster et al., the rate of ET can be modulated by simply changing the pH of the solution since it affects the HOMO levels of the bridge and, therefore, changes the difference between the D−A and bridge energy levels.[25]

Ferrocenoyl oligopeptides have been recently self-assembled into well-organized monolayers on electrodes and used for studies of electron transfer.[20,26−28] The ET between the ferrocene redox probe and the gold surface across an oligopeptide spacer showed a distance-dependent k_{ET} deviating from Marcus-type behavior which was interpreted in terms of a through-bond mechanism.[26]

The present study contributes to the understanding of electron transport through polypeptide molecular bridges. It reveals that for longer peptides the rate of electron transfer is higher than the rate expected for alkanethiol spacers of comparable lengths, which may be due to changes in the secondary structure of the longer oligopeptides. We report on two-component SAMs consisting of redox active oligoglycines inserted into the *n*-alkanethiol matrix. The electroactive components of the monolayers are thiol derivatives containing a cysteamine linker, glycine residues, and a ferrocene headgroup. We studied five systems, which differ in the length of the molecules forming the monolayer: (1) Fc−CO(Gly)$_2$NH−(CH$_2$)$_2$−SH/CH$_3$(CH$_2$)$_8$SH; (2) Fc−CO(Gly)$_3$NH−(CH$_2$)$_2$−SH/CH$_3$(CH$_2$)$_{11}$SH; (3) Fc−CO(Gly)$_4$NH−(CH$_2$)$_2$−SH/CH$_3$(CH$_2$)$_{13}$SH; (4) Fc−CO(Gly)$_5$NH−(CH$_2$)$_2$−SH/CH$_3$(CH$_2$)$_{15}$SH; (5) Fc−CO(Gly)$_6$NH−(CH$_2$)$_2$−SH/CH$_3$(CH$_2$)$_{17}$SH. The properties and the rates of electron transfer through the monolayers were investigated using electrochemical methods.

Experimental Section

Synthesis. The syntheses of Fc−CO(Gly)$_n$NH−(CH$_2$)$_2$−SH ($n = 2-6$) were performed by solid phase synthetic techniques starting from 0.3 mmol·g^{-1} of substituted cysteamine 4-methoxytrityl resin (Novabiochem). Successively, 9-fluorenylmethoxycarbonyl glycines and ferrocenecarboxylic acid (Sigma) were coupled using 1,3-diisopropylcarbodiimide (Sigma) as the coupling reagent. The coupling was monitored by a qualitative ninhydrin test. The cleavage was performed by 5% fluoroacetic acid (Aldrich) in dichloromethane (POCh Gliwice) containing 5% triisopropylsilane (Sigma). The final products were purified by preparative RP-HPLC and then analyzed by ESI-MS.

Preparation of Electrodes. Two-component monolayers were prepared on gold Arrandee substrates. Before adsorption of the monolayer, the substrates were flame annealed in a Bunsen burner. Self-assembly of the mixed monolayers involved incubation of the gold substrates in ethanol solutions containing 0.05 mM of electroactive peptide and 0.95 mM of proper diluent alkanethiol (Aldrich). The deposition was carried out at 35 °C. After 12 h of self-assembly, the modified substrates were rinsed with ethanol and water. Fresh samples were prepared before each experiment.

Electrochemistry. Electrochemical experiments were carried out with a CHI model 660A electrochemical analyzer (CH Instruments Inc.) and an Autolab PGSTAT30 potentiostat (Eco Chemie B. V.) in a three-electrode system. Ag wire was used as a reference electrode, platinum foil as a counter electrode, and the monolayer-coated gold substrate was used as the

* Corresponding author. E-mail: bilewicz@chem.uw.edu.pl.

10.1021/jp049116y CCC: $27.50
Published on Web 05/20/2004

TABLE 1: Structures and Lengths of Molecules[a]

components of the monolayer	structure of oligoglycine[b]	length of the electroactive molecule [Å][c]	length of the nonelectroactive thiol [Å][d]
$Fc-CO(Gly)_2NH-(CH_2)_2-SH/CH_3(CH_2)_8SH$	polyglycine I	12.4	11.6
$Fc-CO(Gly)_3NH-(CH_2)_2-SH/CH_3(CH_2)_{11}SH$	polyglycine I	15.8	15.3
$Fc-CO(Gly)_4NH-(CH_2)_2-SH/CH_3(CH_2)_{13}SH$	polyglycine I	19.3	17.8
$Fc-CO(Gly)_5NH-(CH_2)_2-SH/CH_3(CH_2)_{15}SH$	polyglycine I/polyglycine II	22.7/21.3	20.3
$Fc-CO(Gly)_6NH-(CH_2)_2-SH/CH_3(CH_2)_{17}SH$	polyglycine II	24.4	22.8

[a] The lengths of the molecules were calculated using HyperChem 6.0 assuming the given structure of the oligoglycine spacers (polyglycine I or polyglycine II) and an all-trans conformation of alkanethiols. [b] The torsion angles used for the calculations were $\phi = -139°$, $\psi = +135°$, $\omega = +178°$ for the polyglycine I structure and $\phi = -80°$, $\psi = +150°$, $\omega = +180°$ for the polyglycine II structure. [c] The lengths of the electroactive molecules were calculated as a distance measured from the sulfur atom to the carbonyl group linking molecule with the ferrocene moiety. Bond lengths used in these calculations were S−C, 1.79 Å; C(alkyl)−C(alkyl), 1.54 Å; C(carbonyl)−C(alkyl), 1.52 Å; C(alkyl)−N, 1.47 Å; C(carbonyl)−N, 1.34 Å. [d] The lengths of the alkanethiols were calculated as a distance between the sulfur atom and the terminal carbon atom. Bond lengths used in these calculations were S−C, 1.79 Å; C−C, 1.54 Å.

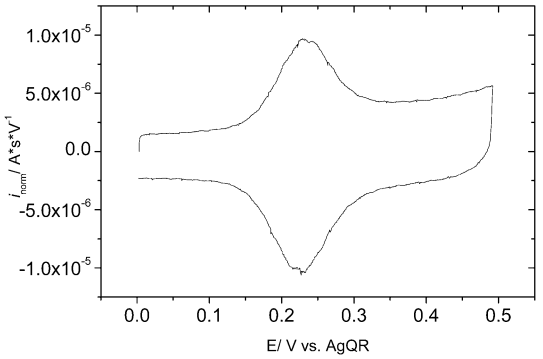

Figure 1. Cyclic voltammogram recorded with a gold electrode modified with a mixed monolayer consisting of $Fc-CO(Gly)_3NH-(CH_2)_2-SH$ and $CH_3(CH_2)_{11}SH$. The supporting electrolyte was 1 M $HClO_4$.

working electrode. The supporting electrolyte was aqueous 1 M $HClO_4$. Water was distilled and passed through a Milli-Q purification system. The resistivity of the final product was 18.2 $M\Omega \cdot cm^{-1}$. All electrochemical measurements were performed at 25 °C.

Results and Discussion

Two-component monolayers were designed assuming that the oligoglycines from dimer up to pentamer adopt the polyglycine I structure, while the hexamer chain forms the polyglycine II helix. This assumption was based on data reported in the literature[29,30] and our FTIR results obtained for oligoglycine samples in the solid state. We also assumed that the conformation of the peptide backbone does not change significantly after adsorption of the oligoglycines on gold. In order to match the components of the mixed monolayers, we calculated the lengths of the electroactive molecules, and then the alkanethiols with the proper chain lengths were selected as the diluents. The difference in length between the spacer separating the ferrocene from electrode surface and the diluent thiol was never larger than 2.4 Å. In the case of mixed monolayers of alkanethiols reported in the literature, the difference between the length of the electroactive component and the diluent is usually in the range of ~0 to 2.3 Å.[9,31−33] Details of the oligoglycine structures and the lengths of the molecules are given in Table 1. Mixed monolayers of alkanethiols and oligoglycines were tested using cyclic voltammetry and electrochemical impedance spectroscopy. These electrochemical methods provide useful information about the properties and electron transfer behavior of the monolayers. Figure 1 presents the cyclic voltammogram recorded for the mixed monolayer consisting of $Fc-CO(Gly)_3NH-(CH_2)_2-SH$ and $CH_3(CH_2)_{11}SH$. The peaks near +0.22 V corresponds to oxidation/reduction of ferrocene redox centers. From the charge under the oxidation peak on the cyclic voltammogram we calculated the percentage of oligoglycine molecules within the monolayer. It was never larger than 3%. The full widths at half-maximum of the peaks (fwhm) at slow scan rates ($\upsilon < 0.2$ V/s) were in the range of 90−100 mV—close to the expected 90.2 mV for an ideal one-electron surface process.[34] This means that the interactions between the neighboring redox sites are negligible. We also found that the values of the capacitance for the mixed monolayers at the double-layer region were in the range of 1.0−3.8 $\mu F/cm^2$. Detailed characteristics of the monolayers are given in Table 2.

The redox kinetics in the mixed monolayers was studied using dc cyclic voltammetry and ac voltammetry. In the case of ac voltammetry, electron transfer rate constants (k^0) for immobilized redox centers were obtained using the treatment proposed by Creager and Wooster.[35] This method involves plotting the ratio of the ac voltammetric peak current to the background current as a function of the logarithm of frequency and then fitting the plot to a calculated curve obtained using the Randles equivalent circuit model (Figure 2). Standard rate constants for monolayers containing longer molecules (with four and more glycine residues) were also determined from Tafel plots obtained from dc cyclic voltammograms. At any point in the voltammogram, the instantaneous faradaic current is given by[36]

$$i_f = nFA(k_c\Gamma_{ox} - k_a\Gamma_{red})$$

For a potential which is 60 mV beyond $E^{\circ\prime}$, the equation can be written as

$$i_f = kQ(t)$$

where $k = k_a$ for the anodic rate constant and k_c for the cathodic rate constant and $Q(t)$ is the charge density corresponding to the quantity of unreacted redox sites on the electrode surface. The rate constant can be calculated by dividing the instantaneous faradaic current by $Q(t)$ at a given potential. As a result, a Tafel plot can be obtained in a single potential sweep experiment. Each rate constant reported here is an average of all measurements (ACV and CV) performed with a given type of monolayer assembly.[37]

If we consider the kinetics of electron transfer through monolayers, the general trend is that as the chains become longer, the rate of electron transfer is lower. This reflects a decrease in the electronic coupling between the redox center and the electrode as the length of the chain linking the redox

TABLE 2: Characteristics of the Monolayers

components of the monolayer	double-layer capacitance [μF/cm^2][a]	surface coverage of electroactive component [%]	full width at half-maximum of the peak [mV]
Fc−CO(Gly)$_2$NH−(CH$_2$)$_2$−SH/CH$_3$(CH$_2$)$_8$SH	3.58 ± 0.42	2.3 ± 1.0	98 ± 4
Fc−CO(Gly)$_3$NH−(CH$_2$)$_2$−SH/CH$_3$(CH$_2$)$_{11}$SH	2.85 ± 0.55	1.4 ± 0.4	99 ± 1
Fc−CO(Gly)$_4$NH−(CH$_2$)$_2$−SH/CH$_3$(CH$_2$)$_{13}$SH	2.07 ± 0.75	1.0 ± 0.6	98 ± 3
Fc−CO(Gly)$_5$NH−(CH$_2$)$_2$−SH/CH$_3$(CH$_2$)$_{15}$SH	1.76 ± 0.55	1.0 ± 0.3	95 ± 4
Fc−CO(Gly)$_6$NH−(CH$_2$)$_2$−SH/CH$_3$(CH$_2$)$_{17}$SH	1.50 ± 0.40	1.0 ± 0.4	95 ± 5

[a] The double-layer capacitance was measured at a potential of 0 V vs AgQR.

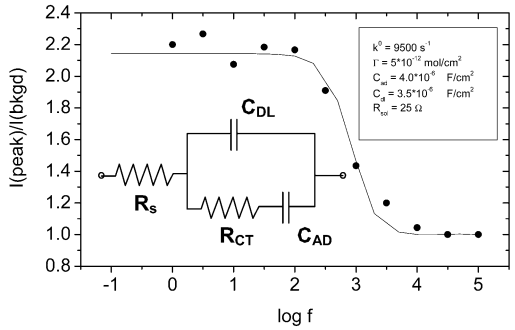

Figure 2. Plot of I(peak)/I(background) vs log(frequency) for a mixed monolayer consisting of Fc−CO(Gly)$_2$NH−(CH$_2$)$_2$−SH and CH$_3$(CH$_2$)$_8$-SH. Points represent experimental data. The solid line is calculated using the equivalent circuit model shown above. C_{dl} is the double-layer capacitance, C_{ad} is the adsorption pseudocapacitance, R_{sol} is the solution resistance, and R_{ct} is the charge transfer resistance expressed as $R_{ct} = (2RT)/(F^2\Gamma k^0)$. The parameters used to calculate the solid fitted line are given in the frame.

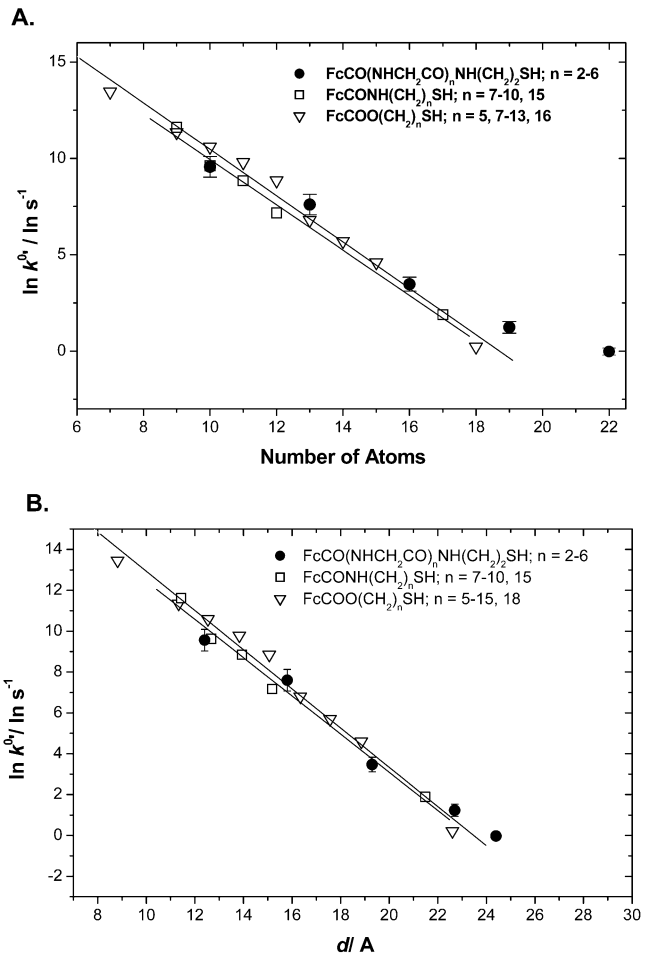

Figure 3. (A) Plot of ln k^0 vs number of atoms in a backbone for mixed monolayers 1−5. The data obtained by Chidsey and co-workers[9,24] (open triangles) and Creager et al.[22] (open squares) for alkanethiolate monolayers with tethered ferrocene redox centers are shown for comparison. Solid lines represents linear fits to distance dependences for *n*-alkanethiolate monolayers. The decay constant for the alkyl chains is about 1.2 per atom. (B) Data from A plotted against the length of the spacer separating the ferrocene from the electrode surface. Lengths of the oligoglycine molecules were taken from Table 1.

center to the electrode surface increases. Similar distance dependence was observed in this study for oligoglycine derivatives. Standard rate constants decreased from 9000 s^{-1} to 1 s^{-1} when the length of the oligoglycine chain was increased from two to six amino acid residues. The plot of ln k^0 versus number of atoms in a backbone is shown in Figure 3. For comparison, we plotted the data obtained by Chidsey and co-workers[9,24] and Creager et al.[22] for alkanethiolate monolayers with ferrocene redox centers (open squares and triangles). The distance dependence of the electron transfer rate through the oligoglycines is similar to those reported for simple *n*-alkanethiols with a tethered ferrocene redox site, but only if we consider molecules containing two to four amino acid residues. The rate constants for short chain oligoglycines have similar values to those observed for alkanethiols, and they follow the same exponential dependence with a decay constant of about 1.05 per atom. This result is reasonable if we take into account that the electron transfer efficiency through the amide moiety is actually the same as for two methylene units. This means that the rate constant through the peptide chain should be similar as for a polymethylene chain containing the same number of atoms in the backbone. Our results indicate that the situation is different if we consider longer oligoglycines containing five or six amino acid residues. In this case, the electron transfer rate is faster than that expected on the basis of extrapolation of the rates for the shorter oligoglycines ($n = 2-4$) and the distance dependence is weaker. Thus there are two domains of electron transfer rate variation with chain length for oligoglycine bridges. Similar results were obtained using a pulse radiolysis technique by Isied and co-workers.[38,39] These authors measured the kinetics of intramolecular electron transfer across oligoproline bridges in synthetic donor−acceptor complexes, and they found that for bridges containing four to six prolines the distance dependence is much weaker than for shorter bridges. The possible reason for this weak dependence is the change in the secondary structure of the peptide bridge, which takes place for longer chains. This transition in secondary structure may contribute to a more efficient pathway through the peptide bridge. Our results may be explained in exactly the same way, assuming that the secondary structure of longer oligoglycines differs from the secondary structure of short chain derivatives. This interpretation can be supported by theoretical investigations recently reported by Shin and co-workers.[40] Their results show that the decay constant for the distance dependence of the electron transfer rate across an oligoglycine bridge is strongly influenced by the secondary structure of the peptide. The value of the decay constant can vary from 0.69 Å^{-1} for the polyproline II structure

to 1.49 $Å^{-1}$ for the polyproline I structure. If we plot the rate constants presented in Figure 3A against the length of the spacer separating the ferrocene from the electrode surface (Figure 3B), our data for oligoglycines fit the data for alkyl bridges. The exception is the rate constant measured for the hexamer, which is slightly higher than expected. This is reasonable if we take into account that the oligoglycines from dimer up to pentamer adopt the polyglycine I structure, while the hexamer chain forms the polyglycine II helix. The latter structure may provide more efficient coupling between the redox site and the metal of the electrode. Thus the distance dependence of the electron transfer observed in our experiments confirms the predictions of Shin and co-workers.[40]

Another possible explanation of the observed distance dependence involves the change of the electron transfer mechanism with increasing molecular length of the peptide bridge. This interpretation is reasonable if we consider the results of theoretical investigations reported by Petrov and May[41] who postulate that the unusual distance dependence observed for oligoprolines arises from the transition between the superexchange mechanism and the sequential one. The latter mechanism becomes more efficient if the molecular length is increased. This means that in our case electron transfer through short chain oligoglycines can occur according to a tunneling mechanism, while for the longer chain ($n = 6$) the hopping mechanism may contribute to the overall electron transport. Morita and Kimura found that the electron transfer through a helical peptide containing 16 amino acid residues is dominated by inelastic hopping.[42] Therefore, the electron transfer rates observed for longer oligoglycines ($n = 5,6$) may reflect changes in the secondary structure but also the "transition region" between the two mechanisms of ET.

Acknowledgment. This work was supported by KBN (Grant No. 3T09A 12219) and MENiS funds within the Project 120-501/68-BW-1602/12/03.

References and Notes

(1) Adams, D. M.; Brus, L.; Chidsey, C. E. D.; Creager, S.; Creutz, A.; Kagan, C. R.; Kamat, P. V.; Lieberman, M.; Lindsay, S.; Marcus, R. A.; Metzger, R. M.; Michel-Beyerle, M. E.; Miller, J. R.; Newton, M. D.; Rolison, D. R.; Sankey, O.; Schanze, K. S.; Yardley, J.; Zhu, X. *J. Phys. Chem. B* **2003**, *107*, 6668.

(2) Siddarth, P.; Marcus, R. A. *J. Phys. Chem.* **1990**, *94*, 2985.

(3) Newton, M. D. *Chem. Rev.* **1991**, *91*, 767.

(4) Liang, C.; Newton, M. D. *J. Phys. Chem.* **1993**, *97*, 3199.

(5) Newton, M. D.; Feldberg, S. W.; Smalley, J. F. Theory and Computational Modeling: Medium Reorganization and Donor−Acceptor Coupling in Electron Transfer Processes. In *Interfacial Chemistry*; Wieckowski, A, Ed.; Marcel Dekker: New York, 1999; pp 97−114.

(6) Beratan, D. N.; Onuchcic, J. N.; Winkler, J. R.; Gray, H. B. *Science* **1992**, *258*, 1740.

(7) Petrov, E. G.; Shevchenko, Y. V.; May, V. *Chem. Phys*. **2003**, *288*, 269.

(8) Holman, M. W., Liu, R.; Adams, D. M. *J. Am. Chem. Soc*. **2003**, *125*, 12649.

(9) Chidsey, C. E. D. *Science* **1991**, *251*, 919.

(10) Becka, A. M.; Miller, C. J. *J. Phys. Chem*. **1992**, *96*, 2657.

(11) Cheng, J.; Saghi-Szabo, G.; Tossel, J. A.; Miller, C. J. *J. Am. Chem. Soc.* **1996**, *118*, 680.

(12) Sachs, S. B.; Dudek, S. P.; Hsung, R. P.; Sita, L.; Smalley, J. F.; Newton, M. D.; Feldberg, S. W.; Chidsey, C. E. D. *J. Am. Chem. Soc.* **1997**, *119*, 10563.

(13) Creager, S.; Yu, C. J.; Bamdad, C.; O'Connor, S.; MacLean T.; Lam, E.; Chong, Y.; Olsen, G. T.; Luo, J.; Gozin, M.; Kayyem, J. F. *J. Am. Chem. Soc.* **1999**, *121*, 1059.

(14) Slowinski, K.; Fong, H. K. Y.; Majda, M. *J. Am. Chem. Soc*. **1999**, *121*, 7257.

(15) Sumner, J. J.; Weber, K. S.; Hockett, L. A.; Creager, S. E. *J. Phys. Chem. B* **2000**, *104*, 7449.

(16) Napper, M. A.; Liu, H.; Waldeck, D. H. *J. Phys. Chem. B* **2001**, *105*, 7699.

(17) Sikes, H. D.; Smalley, J. F.; Dudek, S. P.; Cook, A. R.; Newton, M. D.; Chidsey, C. E. D.; Feldberg S. W. *Science* **2001**, *291*, 1519.

(18) Sek, S.; Misicka, A.; Bilewicz, R. *J. Phys. Chem. B* **2000**, *104*, 5399.

(19) Sek, S.; Bilewicz, R. *J. Electroanal. Chem.* **2001**, *509*, 11.

(20) Sek, S.; Palys, B.; Bilewicz, R. *J. Phys. Chem. B* **2002**, *106*, 5907.

(21) Sek, S.; Moszynski, R.; Sepiol, A.; Misicka, A.; Bilewicz, R. *J. Electroanal. Chem*. **2003**, *550*, 359.

(22) Weber, K.; Hockett, L.; Creager, S. E. *J. Phys. Chem. B* **1997**, *101*, 8286.

(23) Liu, B.; Bard, A. J.; Mirkin, M. V.; Creager, S. E. *J. Am. Chem. Soc.* **2004**, *124*, 1485.

(24) Robinson, D. B.; Chidsey, C. E. D. *J. Phys. Chem. B* **2002**, *106*, 10706.

(25) Walsh, A. D.; Keyes, T. E.; Foster, R. J. *J. Phys. Chem. B* **2004**, *108*, 2631.

(26) Galka, M. M.; Kraatz, H.-B. *ChemPhysChem.* **2002**, *3*, 356.

(27) Bediako-Amoa, I.; Silerova, R.; Kraatz, H.-B. *Chem. Commun.* **2002**, 2430.

(28) Bediako-Amoa, I.; Sutherland, T. C.; Li, C. Z.; Silerova, R.; Kraatz, H.-B. *J. Phys. Chem. B* **2004**, *108*, 704.

(29) Smith, M.; Walton, A. G.; Koenig, J. L. *Biopolymers* **1969**, *8*, 29.

(30) Gupta, V. D.; Gupta, M. K.; Nath, K. *Biopolymers* **1975**, *14*, 1987.

(31) Creager, S. E.; Rowe, G. K. *Anal. Chim. Acta* **1991**, *246*, 233.

(32) Richardson, J. N.; Rowe, G. K.; Carter, M. T.; Tender, L. M.; Curtin, L. S.; Peck, S. R.; Murray, R. W. *Electrochim. Acta* **1995**, *40*, 1331.

(33) Finklea, H. O.; Liu, L.; Ravenscroft, M. S.; Punturi, S. *J. Phys. Chem*. **1996**, *100*, 18852.

(34) Brown, A. P.; Anson, F. C. *Anal. Chem*. **1977**, *49*, 1589.

(35) Creager, S. E.; Wooster, T. T. *Anal. Chem*. **1998**, *70*, 4257.

(36) Finklea, H. O. Electrochemistry of Organized Monolayers of Thiols and Related Molecules on Electrodes. In *Electroanalytical Chemistry*; Bard, A. J., Rubinstein, I., Eds.; Marcel Dekker: New York, 1996; pp 109−335.

(37) The number of measurements was 10−15 for each type of monolayer.

(38) Isied, S. S., Ogawa, M. Y.; Wishart, J. F. *Chem. Rev*. **1992**, *92*, 381.

(39) Ogawa, M. Y.; Wishart, J. F.; Young, Z.; Miller, J. R.; Isied, S. S. *J. Phys. Chem.* **1993**, *97*, 11456.

(40) Shin, Y.-G. K.; Newton, M. D.; Isied, S. S. *J. Am. Chem. Soc*. **2003**, *125*, 3722.

(41) Petrov, E. G.; May, V. *J. Phys. Chem. A* **2001**, *105*, 10176.

(42) Morita, T.; Kimura, S. *J. Am. Chem. Soc*. **2003**, *125*, 8732.